Searching for CesrTA guide field nonlinearities in beam position spectra

Laurel Hales
Department of Physics and Astronomy,
University of Utah, Salt Lake City, Utah, 84112
(Dated: August 14, 2010)

This project consisted of looking for nonlinearities using the beam position spectra for the Cornell Storage Ring. With the intent of finding new ways of locating non-linear errors in the magnet set-up. The main part of this project consisted of examining several different non-linear effects to ensure that they produced the expected results. These effects contribute to two different methods for discovering non-linearities. These effects were tested using both simulations and data from the Cornell Storage Ring. It has been shown that these effects are large enough that they can be seen clearly above the noise level in data from the Storage Ring. These effects can be tested using different lattice arrangements, in order to discover how the lattice arrangement effects these non-linear effects. This in turn can lead to a method for discovering and correcting non-linear errors.

I. INTRODUCTION

Inside of a particle accelerator there are many magnets that direct, focus, and control the beam. Each of these magnets has a specific purpose. The dipole magnets bend the particle beam and keep it inside the accelerator. The quadrupole magnets act as lenses and focus the beam, keeping the particles bunched together. These two magnets are the main optics. The higher order magnets have specific purposes as well. The sextupole magnets are used to correct energy dependent focusing caused by the quadrupoles.

Errors in the magnet setup can make the accelerator less efficient and it can also increase the likelihood of losing the beam. It is important to find ways of being able to detect where the errors in the optics set up are located. Our goal was to explore new ways of looking for non-linear errors in the optics. There are three main causes of non-linear errors. The first cause is that the magnetic optics design is poorly planned. The magnets are configured in such a way that they produce the errors. The second and third causes of non-linear magnets have to do with the magnets themselves. If the magnets are set to the wrong value that will introduce non-linear errors. And even if everything is perfect, and the magnets are all set to the correct values, there will still be errors because they are not ideal magnets. A dipole magnet, for example, will have sextupole errors. If we can locate the cause of these errors than it is possible to correct them by adjusting the values of the magnets. Once these errors are corrected it will make it possible to achieve higher oscillation amplitudes without the increasing the risk of losing the particles. It will also make it possible to reduce bunch shape distortions. Failure to correct these errors increases the likelihood of losing particles.

We have examined two possible methods for detecting non-linear errors. The primary goal of this project was to examine both of these methods and determine if it would be possible to use them. In both of these methods we examined non-linear effects in the beam position spectra. We tested these methods in two ways. First we used a simulated data to determine if we could in fact see the effects that we expected. We then used data from the

storage ring to determine if we would be able to see the same signals above the actual noise level. We tried this with two different lattices in order to make sure that we would still be able to see the effects after the sextupole arrangement was changed.

II. EXAMINING NON-LINEAR EFFECTS

A. Methods

1. Simulation Methods

The simulation used tracking codes from BMAD to determine the path of a particle beam around the storage ring. It followed the course of a particle bunch that was displaced from the normal trajectory by a set amount. Due to the fact that the simulation does not take damping into account, the simulation produced the same results as would have been produced had the particle beam been driven by a sinusoidal shaker. The user of the simulation was able to determine the initial displacement in both the horizontal and the vertical dirctions, the noise level, and the number of turns.

2. Model Independent Analysis

In order to analyse the data we used a model independent analysis program. The program starts with a positon by history matrix, made from the data collected by the beam position monitors.

$$P^T = \frac{1}{\sqrt{T}}(\overrightarrow{p_1}, \overrightarrow{p_2}, ..., \overrightarrow{p_T}) \tag{1}$$

where T is the number of sequential turns and the t-th row vector is

$$\overrightarrow{p(t)} = (x_1(t), y_1(t), x_2(t), y_2(t), ..., x_M(t), y_M(t)) \tag{2}$$

Using the method of Singular Value Decomposition (SVD) we can write the matrix P as the product of three other matricies, T, Λ, and Π

$$P = T\Lambda\Pi^T \tag{3}$$

Where the columns of the T matrix give the time development of the beam trajecetory. The Diagonals of the Λ matrix give the eigenvalues (or the singular values), or the amplitudes of the eigen componants. And the Rows of the Π matrix define the spatial function around the ring. [1]

3. Method 1

Quadrupole and dipole magnets have linear restoring forces. However, a sextupole of strength k_2 adds a nonlinear restoring force:

$$\frac{d^2x}{dt^2} = -\omega^2 x - k_2 x^2 \tag{4}$$

This can be solved in general as:

$$x(t) = x_0 cos(\omega t) + \sum_{m=0}^{2} B_m cos(m\omega t) \tag{5}$$

When that solution for x is plugged into the differential equation above there are multiple powers of cosine.

$$cos^2(\omega t) = \frac{1 + cos(2\omega t)}{2} \tag{6}$$

This leads to multiples of ω. These multiples of ω can be seen as harmonics of the tune in the columns of the τ matrix. The magnitude of these harmonics should be related to the driving amplitude by the following power law dependence: $f_h : \lambda_1 \propto A$; $2f_h : \lambda_2 \propto A^2$; $3f_h : \lambda_3 \propto A^3$;

The harmonics can clearly be seen in the Fourier Transform of the different columns of the τ matrix. This is shown in figure 1.

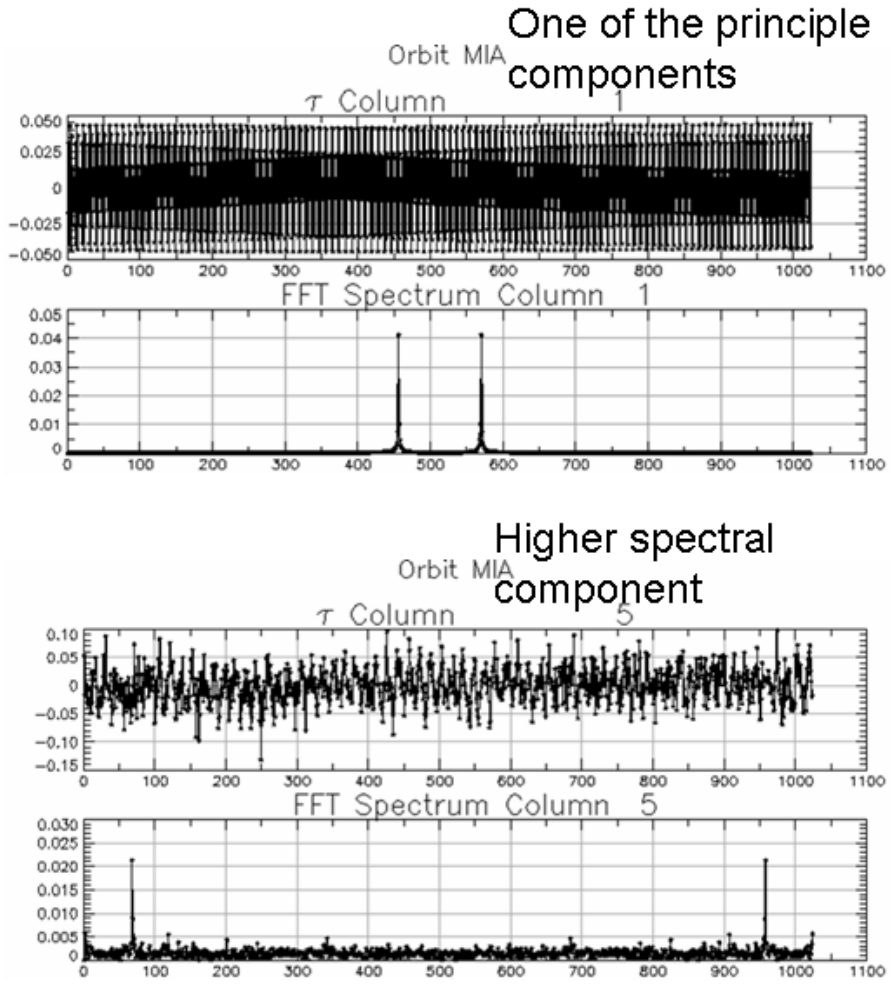

FIG. 1: the graph of two columns of tau and their FFTs.

We decided to measure this effect. The magnitude of the harmonics is proportional to the λ value that corresponds with the τ column in which it appears. We decided to estimate

the magnitude of each harmonic at a point where the β function is thirty-six meters. It is known that: [1]

$$\lambda_+^2 + \lambda_-^2 =< J_t > \sum_{j=1}^{M} \Delta_j^2 \tag{7}$$

Where $< J_t >$ is the average normalized amplitude of the motion and Δ_j^2 is the square of the associated Π matrix elements. From the previous equation we can find:

$$\lambda_+^2 + \lambda_-^2 =< J_t > \sum_j \beta_{Aj}\gamma_j^2 \tag{8}$$

$$\approx< J_t > \sum_j \beta_{Aj} \tag{9}$$

$$=< J_t > M < \beta_{BPM} > \tag{10}$$

given that M is the number of BPMs and that $< \beta >= 18$ meters we get:

$$< J_t >= \frac{\lambda_+^2 + \lambda_-^2}{M < \beta_{BPM} >} \tag{11}$$

from that we find:

$$\hat{x} = \sqrt{\beta_x < J_t >} \tag{12}$$

$$= \frac{\sqrt{\lambda_+^2 + \lambda_-^2}\sqrt{2}}{\sqrt{M}} \tag{13}$$

Unfortunately, this method only works when there are only a sine-like and a cosine-like term, associated with λ_+ and λ_- However, sometimes this is not the case, and there are more than two terms for each harmonic. When this is the case we used the following method to find the magnitude of each harmonic: We start with:

$$amplitude = \sqrt{(\hat{\tau}_+\lambda_+\pi_{m+})^2 + (\hat{\tau}_-\lambda_-\pi_{m-})^2} \tag{14}$$

from that we get

$$\hat{x} = \sum_{i=1}^{N} a_i \, (\, cos\theta_i sin\theta_i \,) \tag{15}$$

$$t^2 = a^2 + b^2 + (2ab)cos(\theta_1 - \theta_2) \tag{16}$$

$$t^2 \approx a^2 + b^2 \tag{17}$$

because $1/2\pi \int_0^{2\pi} cos\theta \, d\theta = 0$. Due to the principle of random walk we decided to add a factor or $1/N$ where N is the number of τ columns where that harmonic appears. This gives us

$$\hat{x}^2 = \frac{1}{N} \sum a_i \tag{18}$$

where

$$a_i = \tau_i \lambda_i \pi_j \approx 6\tau_i\lambda_i \tag{19}$$

4. Method 2

$\beta(s)$ is the amplitude function. This modulates the amplitude of the oscilation. The oscillation envelope is described by

$$\hat{x} = \sqrt{\beta J} \tag{20}$$

When a particle beam goes through a sextupole magnet, the magnet can distort the phase space ellipse (refer to fig 2). It can be distorted in such a way that it is no longer even an ellipse.[2] These distortions change the equillibrium value of β. β changes in such a way that

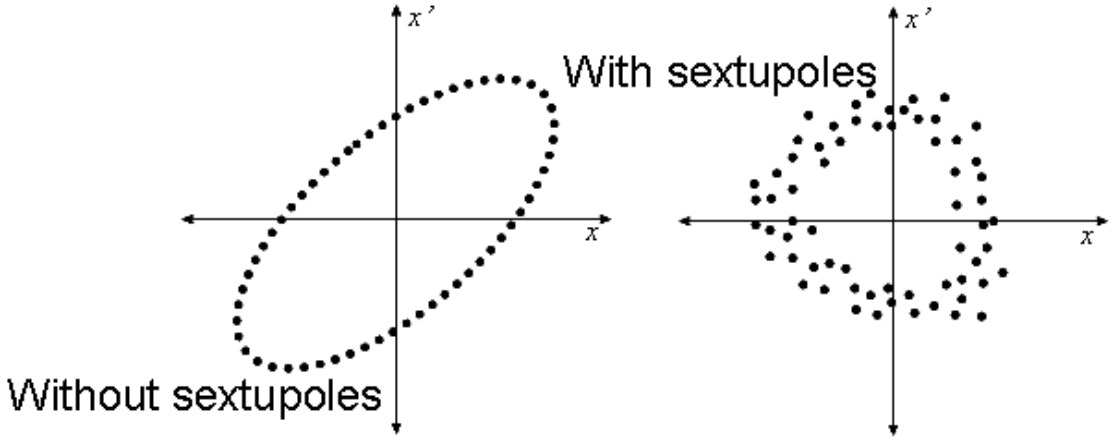

FIG. 2: The effect of sextupole magnets on the phase space ellipse.

its fraction change is proportional to the driving amplitude.

$$\frac{\Delta\beta}{\beta} \propto A \tag{21}$$

A change in β leads to a change in the phase of the oscillation

$$\phi = \int_{s_1}^{s_2} \frac{1}{\beta(x)}\, dx \tag{22}$$

$$\Delta\phi = \int_{s_1}^{s_2} \frac{1}{\beta(x)} \left(\frac{-\Delta\beta(x)}{\beta(x)} + \frac{\Delta\beta^2(x)}{\beta^2(x)} - ...\right) dx \tag{23}$$

$$\approx \int_{s_1}^{s_2} \frac{1}{\beta(x)} \frac{\Delta\beta(x)}{\beta(x)}\, dx \tag{24}$$

A phase shift over the entire ring leads to a tune shift.

$$\Delta Q = \frac{\Delta\phi}{2\pi} \approx \left(\frac{\Delta\beta^2(s)}{\beta^2(s)}\right) \tag{25}$$

This is a second order effect. The sum of the first order deviations around the ring goes to zero. However, the second order effect leads to a tune shift that is quadratically dependent on the driving amplitude. Method two consisted of determining the tune of the oscillation at multiple driving amplitudes in order to examine the dependence on the driving amplitude.

This was examined using MIA analysis. The location of the peak in the FFT of the first τ column gives the fractional tune. Using a parabolic approximation and the three data points closest to the peak of the FFT we estimated the location of the peak and used that to generate a fairly accurate estimation of the fraction tune. When this was done to several different tests with different driving amplitudes or different initial displacements then we could examine the quadratic dependence.

B. Results

1. Results from Method 1

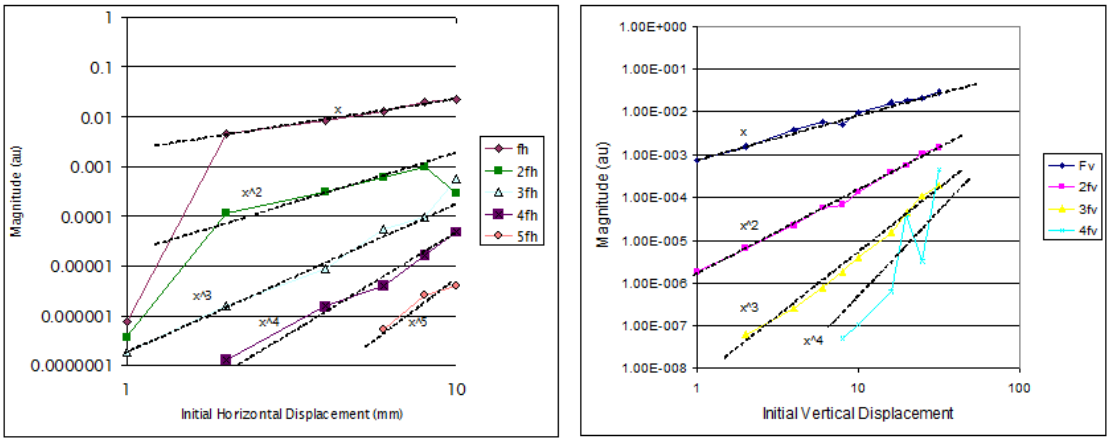

FIG. 3: The relationship between the log of the magnitude of the different harmonics and thel log of the initial displacement for a horizontally displaced sample (left) and a vertically placed sample (right) The dotted lines represent the different power laws as labeled.

The vertically displaced data displays the power law dependence that we expected. The Horizontal data does not display the dependence as well as expected. Possible reasons for this are discussed in a later section. After we showed that it was possible to see the expected effect in simulated data we then used data from the actual storage ring to determine if the same effects could be seen above the level of the noise. The magnitude of the f_h signal is linearly dependent on the driving amplitude. This is clearly shown in both of the lattices. Unfortunately, it is difficult to tell with the other harmonics. As there are not enough data points to be able to see the power law dependence with very much certainty. We are not yet sure why the f_v in the altered lattice seems to have a quadratic dependence. Since there are only three points available, and at least one of them has a small signal, we believe that an acceptable explaination is that there are simply not enough data points present. If we were to have more points then they may show a linear dependence as we expect. As shown above above, the machine data displays generally the same effects as the simulation data .

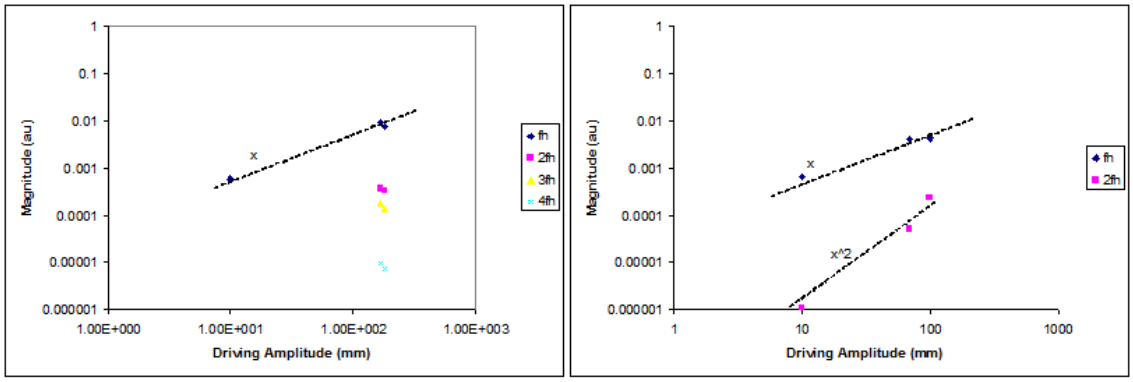

FIG. 4: The relationship between the magnitude of the different harmonics and the oscillation amplitude for a horizontally displaced sample in an unchanged lattice (left) and in a lattice with one changed sextupole (right).

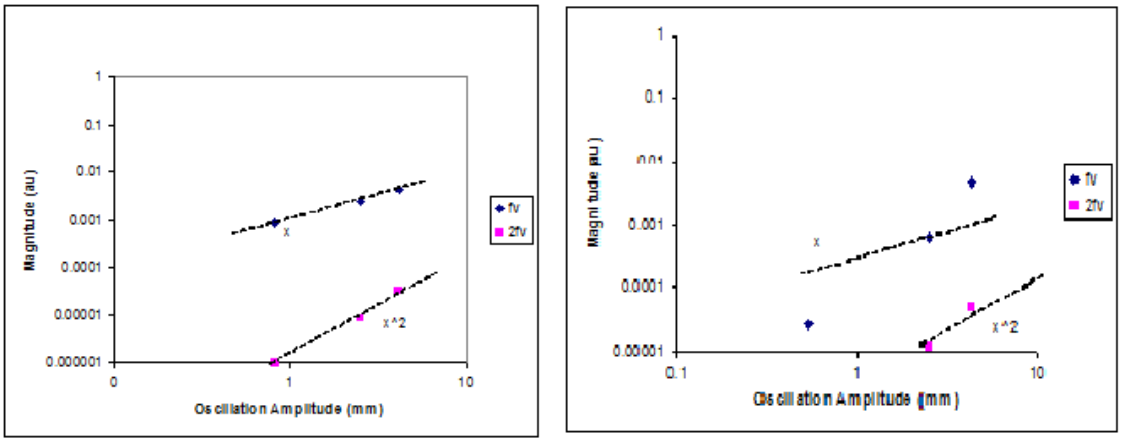

FIG. 5: The relationship between the magnitude of the different harmonics and the oscillation amplitide for a vertically displaced sample in an unchanged lattice (left) and in a lattice with one chaanged sextupole (right)

2. Results from Method 2

The vertically driven bunch clearly shows the expected quadratic relation. However, the horizontal case is not as clear. One possible reason for this is that tthe tunes are nearing a resonance. This will be further discussed in the next section. These charts show the observed relation between the fractional tune and the driving amplitude. Again, we notice that there are not enough data points to clearly display what that relation is. This data also raises another important point. The sign of the relation is not the same as it was for the vertically displaced simulated data. The simulated data had a positive relationship, however, the vertically driven machine data seems to have a netative relationship. This is evidence that there are errors in the machine. This difference in sign is evidence that the actual magnet configuration is not the same as the designed configuration.

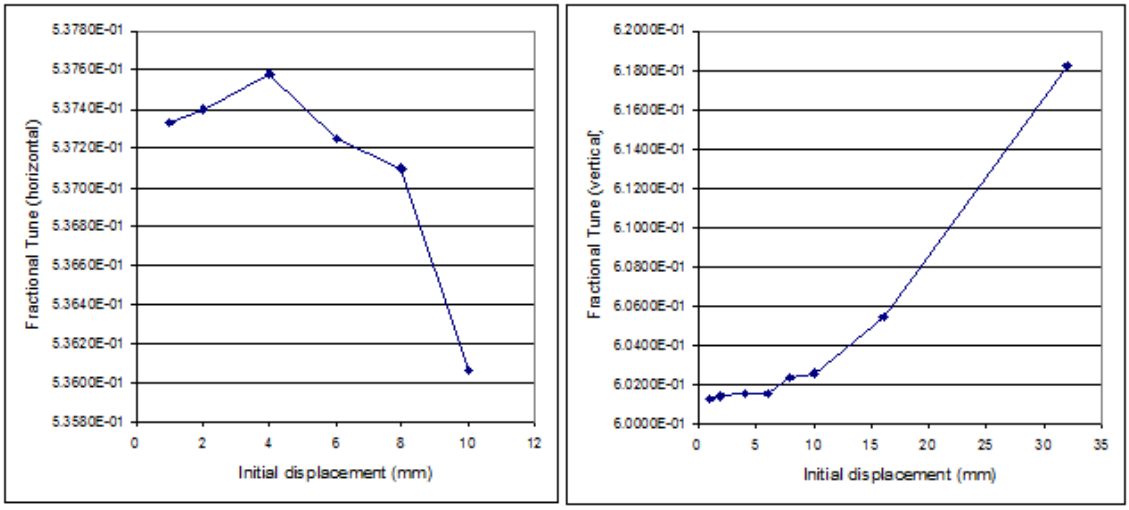

FIG. 6: The simulation data showing the quadratic relation between the fractional tune shift and the initial displacement for a horzontally displaced bunch (left) and a vertically displaced bunch (right)

3. The Possibility of a Resonance

The simulation results for the horizontal data from both Method 1 and Method 2 are not as clear as the results for the data with a vertical displacement. One possible cause for this is that the tune may be approaching a resonance. The tune is in fact approaching two resonances: $2(Q_h)+3(Q_v)+2(Q_s)=3$ and $3(Q_v)+3(Q_s)=2$. Approaching close to a resonance would explain why the data was not what we expected. These simulated experiments are sensitive to even relatively weak resonances due to the fact that there is no damping in the simulated data. The particle beam is sensitive to higher order resonances that may not be seen in the machine.

C. Conclusions

We have shown that it is possible to detect the expected non-linear effects. They are large enough that they are visible in the data from the actual storage ring. We have shown that the effects are in fact what we expected. The magnitude of the different harmonics is in fact related to the driving amplitude by the expected power law. We were not able to show that the quadratic dependence of the tune shift on the driving amplitude in the data from the storage ring, however, we were able to show that in simulations, the dependence is quadratic and we were able to show that a tune shift is visible in data from the storage ring. When more data is collected we expect to be able to show the expected quadratic relation.

D. Future Work

The ultimate goal is of course to create a process that would allow one to use these methods to detect non-linear errors and their placement in the storage ring. This could be an extremely useful tool in optimising the optics. This will entail studying different lattice

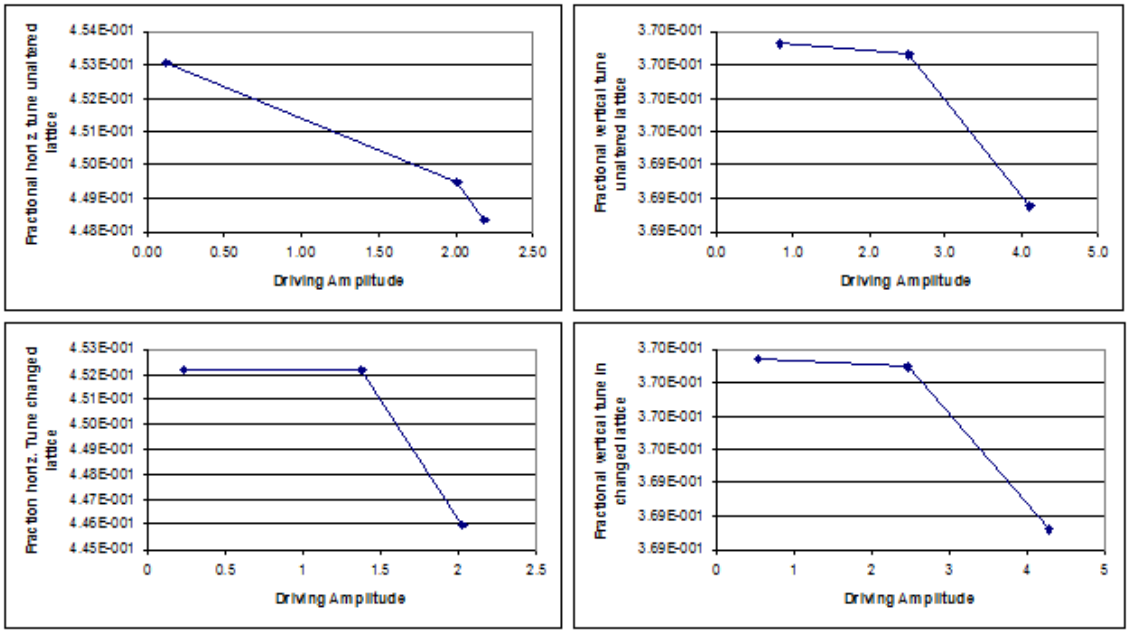

FIG. 7: The relationship between the fractional tune and the ascillation amplitude for four different experiments. Horizontally driven in an unchanged lattice (top left), vertically drivien in an unchanged lattice (top right), horizontally driven in an altered lattice (bottom left), and vertically drive in an altered lattice (bottom right.)

arrangements to discover how the sextipoles can change the effects described above, as well as creating a modeling process that will allow the user to discover where in the ring the non-linear errors are generated. Another possible idea for the future is to consider using an analysis method similar to the one used in Lee et al. [3] for the purpose of lowering the noise level in the signal.

III. ACKNOWLEDGEMENTS

Many thanks to my advisors Dr. Mike Billing Dr. Mark Palmer of Cornell University for their help, support, and patience as I worked through this project. I would also like to thank Heather Williams for her patience as she helped me understand the computer as well as her willingness to answer my questions. Thanks also to those whose efforts made the REU program possible including Georg Hoffstaetter, Ivan Bazarov, Lora Hines, Monica Wesley, and others. This work was supported by the National Science Foundation REU grant PHY-0849885 as well as NSF grant PHY-0734867 and DOE grant DE-FC02-08ER41538.

---

[1] M. Billing, M Forester, H. Willims *Model Independent Analysis of a Circular Accelerator in Transversely Coupled Beam Coordinates* (unpublished)

[2] Klaus, W. (2000). The Physics of particle accelerators. London, UK: Oxford University Press.

[3] X. Pang and S.Y. Lee Appl. Phys. Lett. **106**, 074902 (2009).